Simple Binning Algorithm and SimDec Visualization for Comprehensive Sensitivity Analysis of Complex Computational Models

M. Kozlova[1], A. Ahola[2], P. Roy[3], and J. S. Yeomans[4] *

[1] LUT Business School, LUT University, Lappeenranta 53850, Finland
[2] Laboratory of Steel Structures, LUT University, Lappeenranta 53850, Finland
[3] Vienna, Austria
[4] Schulich School of Business, York University, Toronto, Ontario M3J 1P3, Canada

ABSTRACT. Models of complex environmental systems inherently contain interactions and dependencies among their input variables that affect their joint influence on the output. Such models are often computationally expensive and few sensitivity analysis methods can effectively process such complexities. Moreover, the sensitivity analysis field as a whole pays limited attention to the nature of interaction effects, whose understanding can prove to be critical for the design of safe and reliable systems. In this paper, we introduce and extensively test a simple binning approach for computing sensitivity indices and demonstrate how complementing it with the smart visualization method, simulation decomposition (SimDec), can permit important insights into the behaviour of complex models. The straightforward binning computation generates first-, second-order effects, and a combined sensitivity index, and is considerably more computationally efficient than the "industry standard" measure for Sobol' indices introduced by Saltelli et al. The cases vary from business and engineering to environmental applications. The totality of the sensitivity analysis framework provides an efficient and intuitive way to analyze the behaviour of complex environmental systems containing interactions and dependencies.

Keywords: global sensitivity analysis, SimDec, computational efficiency, environmental decision-making, decision support

1. Introduction

Models of complex environmental, technological, and social systems are characterized by a high degree of complexity and specificity (Yeomans, 2020). While the researchers developing them are experts in such specific mathematical approaches as finite element methods, structural reliability and integrity modeling, and fitness-for-service (prEN 1993, 2023; Mahadevan and Ni, 2003; Shittu et al., 2021; Shen et al., 2023), their professional expertise is frequently deficient in the mathematically comprehensive field of sensitivity analysis (SA) (Saltelli et al., 2019). Potential errors in the underlying structural analysis models can lead to failures that cause catastrophic consequences in service. To prevent such outcomes, it is essential to conduct an effective SA on those models. Furthermore, SA can also be used in model development to identify the most important parameters and their interactions and guide the process. SA can be used to explicitly test the models and exclude those parameters that do not significantly affect uncertainty in the outputs to build simplified approaches. The development of straightforward and intuitive SA approaches is paramount for incorporating SA into standard practice to fully complement the pro-

cesses of building and analyzing a computational model (Saltelli et al., 2019; Iooss et al., 2022). Although the theory of SA has taken major strides forward (Saltelli et al., 2021), their comprehensive employment in "real world" environmental analysis has remained sorely lacking (Saltelli et al., 2019, Kozlova et al., 2024b).

Consequently, this paper provides several contributions to SA for assessing the behaviour of disparate complex models and, in particular, for how to incorporate fundamental SA procedures into environmental analysis in a practical fashion. Firstly, we introduce a novel intuitive procedure that efficiently computes global variance-based sensitivity indices for a given dataset (Section 2), together with its motivation presented (Section 1.1). Secondly, in contrast to recent mathematical developments (Mara et al., 2015; Lamboni and Kucherenko, 2021; Barr and Rabitz, 2023; Borgonovo et al., 2024; Ehre et al., 2024), the new approach is shown to capture dependent inputs automatically while simultaneously revealing several interesting properties that enable examination of the relationships between dependency and interaction (Section 4). Thirdly, the entirety of modern sensitivity analysis literature has focused solely on the computation of sensitivity indices (Menz et al., 2021; Barr and Rabitz, 2023; Di Maio et al., 2023; Jung and Taflanidis, 2023; Shang et al., 2023; Shi et al., 2023; Vuillod et al., 2023; Wang and Jia, 2023; Jia and Wu, 2024). In contrast, we strongly advocate for the concurrent use of visualizations to investigate the

---

shape of the effects in addition to their strength (Section 1.2) and illustrate this with a structural reliability model that possesses nested heterogeneous interaction effects that could not be uncovered without such visual representation (Section 5). Overall, this paper introduces a simple but very powerful framework for the SA of computational models, that computes sensitivity indices to prioritize the input factors followed by a smart visualization for communicating the nature of the discovered effects. There are open-source codes in several programming languages that implement the entire framework to accompany the article (Kozlova et al., 2023; Roy and Kozlova, 2024).

1.1. Sensitivity Indices Computation

Understanding the behaviour of computational models forms the basis for all design and decision-making. The decision-maker obtains information on: what sources of uncertainties are most crucial and might require protection against; which actionable parameters make the most difference and thus represent the perfect levers for managing the system; and, which model parameters create the most noise and require clarification to obtain a clearer representation of the system being modeled.

The sole purpose of the scientific field of SA is to identify which input variables affect the output(s) the most in the computational models (Saltelli et al., 2008). For educational purposes, the conceptual idea behind the sensitivity indices is often explained using scatter plots (Caers, 2018; Saltelli, 2023) as depicted in Figure 1, borrowed from one of the talks devoted to SA (Saltelli, 2023).

Figure 1 displays the intuition behind the variance-based sensitivity indices: namely, bin the X, compute the average of Y in every bin, compute the variance of these average values of Y, and divide the resulting conditional variance to the total variance of Y to obtain the sensitivity index value. Quite unexpectedly, however, the two rare methods that employed this logic Kucherenko et al. (2017); Marzban and Lahmer (2016) have

not been adopted into the usage by the sensitivity analysis community. Among the widely used methods for computing sensitivity indices: some involve game theory (Shapley, 1953) and some Fourier analysis (FAST) (Cukier et al., 1973); the classic Sobol' indices (Sobol', 1993; Homma and Saltelli, 1996; Saltelli, 2002; Saltelli et al., 2010) require juggling multiple simulation matrices; some methods employ polynomial chaos expansion (Sudret, 2008; Crestaux et al., 2009); there is a so-called moment-independent measure which is based on quantifying the shift in the distribution of the output caused by an input (Borgonovo, 2007); some are based on derivatives (Sobol' and Kucherenko, 2010; Kucherenko and Song, 2016); there is a variogram-based method (VARS) (Razavi and Gupta, 2016); while the most recent approach utilizes discrepancy measures (Puy et al., 2024) to quantify the difference between the cumulative probability distributions of simulated data and its running averages. Modern research on sensitivity analysis is actively developing and predominantly targets an increase in the computational efficiency of these various methods (Saltelli et al., 2021; Iooss et al., 2022).

A straightforward method that follows the logic of Figure 1 was independently introduced by Marzban and Lahmer (2016) as a conceptual implementation of Sobol' indices and by Kucherenko et al. (2017) as the double loop rendering method or DLR. Our focus is drawn to this method because: it is intuitive and works precisely as sensitivity indices are conceptually introduced (Figure 1); it is more computationally efficient and more accurate than other methods for estimating Sobol' indices (Kucherenko and Song, 2017); it works with a given dataset. As Plischke (2012) notes, for such methods:

(1) No access to the model is required.

(2) They can work on measured data; and as a result.

(3) The method is indifferent to distribution types and sampling methods. Furthermore, it enables smoother passing of information between the model and sensitivity analysis, if they are performed in different software or by different people.
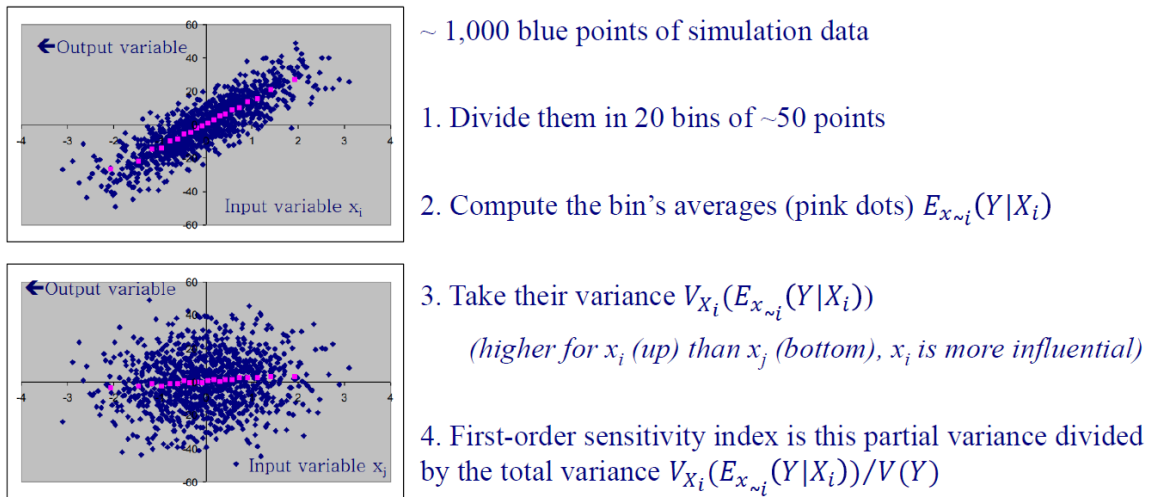

~ 1,000 blue points of simulation data

1. Divide them in 20 bins of ~50 points

2. Compute the bin's averages (pink dots) $E_{x_{\sim i}}(Y|X_i)$

3. Take their variance $V_{X_i}(E_{x_{\sim i}}(Y|X_i))$

   (higher for x_i (up) than x_j (bottom), x_i is more influential)

4. First-order sensitivity index is this partial variance divided by the total variance $V_{X_i}(E_{x_{\sim i}}(Y|X_i))/V(Y)$

Figure 1. Conceptual representation of the sensitivity indices, adapted from (Saltelli, 2023).

This paper extends this concept to explicitly capture the second-order effects. Such an approach has not been considered previously, as Marzban and Lahmer (2016) algorithm determined the first-order effects, exclusively, while Kucherenko et al. (2017) estimated the first-order and the total effects. This modified new approach, referred to as the Simple binning approach (SBA), introduces additional benefits:

(1) The choice of the number of bins is no longer the user's responsibility, it is automated based on experiments by Marzban and Lahmer (2016).

(2) It works with dependent inputs (although developments that allow sensitivity analysis of models with dependent input variables exist (Lamboni and Kucherenko, 2021; Mara et al., 2015; Da Veiga, 2015; Borgonovo et al., 2024; Ehre et al., 2024), majority of them require certain additional transformations, whereas the SBA captures dependent inputs "as is" (Kucherenko et al., 2017) and preserves the conservation property).

(3) The measure for the second-order effect allows studying the behaviour of dependent inputs that affect the output interactively, revealing dependency-interaction intertwining.

(4) It works with categorical/discrete variables.

(5) It is resistant to different numbers of observations in bins due to the usage of weighted variance.

(6) As a result, it can work with empirical datasets.

(7) It can be used to quantify the sensitivity of the output to intermediate outputs in simulation models.

1.2. Importance of Visualization

The modern practice of sensitivity analysis systematically stops at computing sensitivity indices (Menz et al., 2021; Barr and Rabitz, 2023; Di Maio et al., 2023; Jung and Taflanidis, 2023; Shang et al., 2023; Shi et al., 2023; Vuillod et al., 2023; Wang and Jia, 2023; Jia and Wu, 2024) and does not take an additional step of investigating the shape of the effects in a model. Model interactions may arise in many different forms, particularly in environmental systems (Kozlova et al., 2024a). In one model, they might be the result of multiplication in which the effect of one input variable linearly increases in the higher values of another input variable. In another model, the effect of the variable might be strong in a certain region of another input variable, but negligible in the others. The direction of the influence of one input factor on the output might be flipped in different regions of another input variable. In all of these cases, the sensitivity index will show a positive second-order effect of a certain degree, but no more. Namely, no indication of the type of interaction effect can be obtained through sensitivity indices alone (Kozlova at al., 2024b).

However, explicit knowledge of the nature of interaction effects is crucial for effective decision-making and engineering design and, thus, visualization of the effects is a "must-have" practice for computational model analysis. Heat maps (Pleil et al., 2011; Owen et al., 2019) and response surfaces (Myers et al., 2016) are inherently three-dimensional visualizations that can portray the joint effect of a pair of input variables on the model output. However, these visualization types cannot handle simultaneous variations of multiple inputs and, thus, fail to depict higher-order interactions.

These visualization limitations are overcome by the simulation decomposition (SimDec) approach in a variety of applications (Kozlova and Yeomans, 2020, 2022b; Kozlova et al., 2024b, 2024c). SimDec partitions the output probability or frequency distribution into sub-distributions comprised of combinations of specific regions of influential input variables, thereby exposing the nature of interaction effects (Kozlova et al., 2024b, 2024c). The SimDec approach has demonstrated value in multiple environmental contexts (Kozlova and Yeomans, 2019; Deviatkin et al., 2021; Liu et al., 2022). In this paper, it will be shown that the concurrent employment of the SBA to identify the most influential input variables with SimDec to display the nature of those effects results in a simple-to-implement, intuitive, and sophisticated framework for conducting SA. Various examples are used to convey the diverse behaviours that can be revealed by quantitative measures of the new SA approach, including the earlier carbon capture model of Kozlova and Yeomans (2019) that has its previous visualization-only analysis significantly enhanced through the additional credibility provided by the concurrent computation of the SBA sensitivity indices.

2. Simple Binning Approach to Sensitivity Indices

2.1. Existing Approach for First-Order Effects

Marzban and Lahmer (2016) and Kucherenko et al. (2017) introduced a conceptual implementation to Sobol' first-order indices. Unlike the specific design of experiments normally need ed for computing the estimators of Sobol' indices (several sets of Monte Carlo simulation data with different input variable(s) fixed) (Saltelli, 2002; Saltelli et al., 2010), their approach requires only a single Nobservations $*$ Kinputs dataset generated from one Monte Carlo simulation. The approach involves binning along the X's range, computing averages of Y's within every bin, and then taking the variance of those averages (as shown in Figure 1). The first-order sensitivity index is then computed as the conditional variance divided by the variance of Y, according to the formal description of Sobol' indices (Sobol', 2001):

$$S_{x_i} = \frac{Var(IE(Y \mid X_i))}{Var(Y)} \qquad (1)$$

Kucherenko et al. (2017) also provide an algorithm for the estimation of the total effects (the effects of individual input variables containing all their interactions) and demonstrate that the method is able to handle dependent inputs. Kucherenko and Song (2017) subsequently ran multiple tests that conclusively demonstrate that this method is more computationally efficient and more accurate than other estimators.

To estimate the number of bins, Kucherenko and Song (2017) propose a "rule of thumb" $\sim \sqrt{N_{obs}}$, while Marzban and Lahmer (2016) define the optimal number of bins for different Nobs and Kinputs, which results in more conservative

Table 1. Recommendations for The Choice of The Number of Bins

Number of observations, N_{obs}	$\sqrt{N_{obs}}$	Number of input variables (K_{inputs})		
		3	6	12
1,000	32	10	10	10
2,500	50	25	10	10
5,000	71	50	10	10
7,500	87	50	25	10
10,000	100	50	50	10
25,000	158	100	50	25
50,000	224	100	50	50

Note: By Kucherenko and Song (2017) (second column) and Marzban and Lahmer (2016) (other columns).

estimates for this parameter, Table 1.

A smaller number of bins results in less noisy estimates for sensitivity indices. Therefore, the number of bins recommendation of (Marzban and Lahmer, 2016) is followed in the subsequent SBA code implementation and automated with linear fitting clamped at 10:

$$m_{bins} = \left\lceil \begin{array}{l} 36 - 2.7 \times K_{inputs} + (0.0017 - 0.00008 \times K_{inputs}) \\ \times N_{obs} \end{array} \right\rceil$$

$$M_{bins} = \begin{cases} m_{bins}, & if\ m_{bins} < 30 \\ 10, & otherwise \end{cases} \quad (2)$$

2.2. Extension to Second-Order Effects

Building upon the first-order index calculation approach, we extend the binning concept into the computation of second-order effects. To accomplish this extension, instead of binning a line defined by a single input, we must now bin a two-dimensional area defined by two inputs. Figure 2.
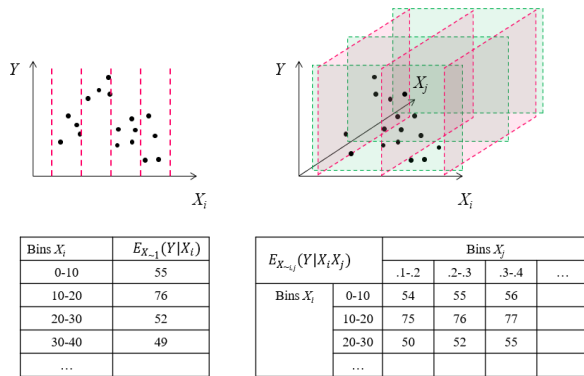
Figure 2. SBA for first-order indices (left) and second-order indices (right).

The calculation steps follow an analogous procedure for computing averages in the bins and their variance, except we employ a weighted variance to account for possibly unequal numbers of observations in bins relevant to categorical varia-

bles with different frequencies for different categories, and for second-order effects:

$$Var_w(Y_{x_i}) = \frac{\sum_{b=1}^{N_{bins}} N_{obs_b} (\overline{Y_b} - \overline{Y})^2}{\sum_{b=1}^{N_{bins}} N_{obs_b}} \quad (3)$$

where the binning happens over X_i and the averages are taken of Y values as illustrated in Figure 2. The second-order effect is defined in the classic way (Saltelli, 2002):

$$S_{x_i x_j} = \frac{Var(IE(Y|X_i, X_j))}{Var(Y)} - S_{x_i} - S_{x_j} \quad (4)$$

or

$$S_{x_i x_j} = \frac{Var(IE(Y|X_i, X_j))}{Var(Y)} - \frac{Var(IE(Y|X_i))}{Var(Y)}$$
$$- \frac{Var(IE(Y|X_j))}{Var(Y)} \quad (5)$$

The number of bins is defined based on the optimal number of observations per bin. For the first-order effects, the number of bins is a linear approximation of the optimal experimental number of bins as a function of the number of simulation runs and the number of inputs, Equation (2). For the calculation of second-order effects, to preserve approximately the same number of observations in two-dimensional bins, the range of each input variable is broken down into a number of intervals $M_{bins_{soe}}$ equal to a square root (rounded to the nearest integer) of the previously computed number of bins for the first-order effects:

$$M_{bins_{soe}} = \left\lceil \sqrt{M_{bins}} \right\rceil \quad (6)$$

The same number of bins should be applied to all terms in Equation (5). For example, a stylized scheme in Figure 2 depicts four bins for X_i for the first-order effect, which translates into two bins for X_i and two for X_j for second-order effects, thus, the bin size remains the same.

An aggregate or combined sensitivity index (also known as a closed index) can now be calculated which, for each input variable, sums up its first-order effect and halves of second-order indices with all other input variables:

$$S_{combined_{x_i}} = S_{x_i} + \sum_{\substack{j=1 \\ i \neq j}}^{K_{inputs}} \frac{S_{x_i x_j}}{2} \quad (7)$$

This combined sensitivity index aggregates the individual and the interaction effects of each input variable. The sum of combined indices for all model input variables would equal 1 if there are no effects higher than second-order in the model and

no unaccounted variation. However, due to the approximation nature of the method, potentially noisy results due to binning (Marzban and Lahmer, 2016), and the imperfections of sampling, the sum of combined sensitivity indices can deviate slightly from 1 even in the absence of higher-order effects. Irrespectively, we advocate for the usage of this approach in combination with SimDec to determine the selection of the prime input variables for decomposition. As long as the ranking of inputs' importance is preserved, noise does not prove to be an impediment.

3. Testing the SBA

3.1. Capturing Interactions – The Portfolio Model

To demonstrate the efficacy of the SBA in capturing second-order effects, we examine a portfolio model presented in the seminal sensitivity analysis textbook by Saltelli et al. (2004). At the heart of the portfolio model are summations and multiplications which are basic operations in any computational model. The model equation and the input distributions are as follows:

$$Y = C_s P_s + C_t P_t + C_j P_j \tag{8}$$

where $P_s \sim N(0; 4)$, $P_t \sim N(0; 2)$, $P_j \sim N(0; 1)$, $C_s \sim N(250; 200)$, $C_t \sim N(400; 300)$, and $C_j \sim N(500; 400)$.

The mainstream evaluation of Sobol' sensitivity indices is based on the proposed by Saltelli estimator (Saltelli, 2002; Saltelli et al., 2010) and open-sourced in the Python library for sensitivity analysis SALib. A side-by-side comparison of Sobol' sensitivity index results obtained by the Saltelli implementation (Saltelli, 2002) as reported in Saltelli et al. (2004) and the new SBA are presented in Table 2.

Table 2. Comparison of the Sobol' Indices Obtained by the Saltelli Implementation (Saltelli, 2002) and SBA on A Portfolio Model

Effect	Sobol'	Conceptual implementation	Delta
First-order effects			
Ps	36 %	35 %	−1 %
Cs	0 %	1 %	1 %
Pt	22 %	20 %	−2 %
Ct	0 %	1 %	1 %
Pj	8 %	8 %	0 %
Cj	0 %	2 %	2 %
Sum of first-order effects	66 %	67 %	1 %
Second-order effects			
PsCs	18 %	16 %	−2 %
PtCt	11 %	10 %	−1 %
PjCj	5 %	6 %	1 %
Sum of second-order effects	34 %	32 %	−2 %
Total effects	100 %	99 %	−1 %
Model evaluations	21,000	1,000	

Table 2 demonstrates that the SBA produces meaningful

sensitivity indices close to the Saltelli implementation of the Sobol' indices (Saltelli, 2002). However, the SBA used only 1,000 model evaluations, while 21,000 data points were required to compute the Saltelli measure. The number of bins used was ten for first-order effects and three for second-order effects.

The indices produced by both approaches in Table 2 are based on limited model evaluations with simple random sampling. Because different simulation runs can generate to some degree different datasets, we repeated the exercise 1,000 times to ascertain how stable the index estimations were. Figure 3 provides a comparison of the results obtained with the Saltelli implementation and the SBA for two sampling sizes. The sample size for the Saltelli implementation is dependent on the number of inputs analyzed K and the specificity of the approach of fixing factors in the simulation matrices following the equation $N = n \times (2K + 2)$, where n should be a power of two. The two sample sizes chosen are $N = 128 \times (2 \times 6 + 2) = 1792$ and $N = 1024 \times (2 \times 6 + 2) = 14336$. The SBA produces more accurate estimates than the Saltelli implementation of Sobol' indices, even if the larger sample for the latter is contrasted with the smaller sample for the former.

In addition, we compared how the SBA performs with (i) simple random sampling (Olken and Rotem, 1986; Singh and Singh, 2003), which is often used for Monte Carlo simulation, (ii) quasi-random sampling (Sobol', 1967; Owen, 2023) with the Sobol' low discrepancy sequence, which is reportedly a more efficient sampling strategy that fills the space more uniformly (Kucherenko et al., 2015), and (iii) full factorial design, frequently used in engineering contexts (Tong, 2006; Alidoosti et al., 2013; Suard et al., 2013) (see Figure 4). For this experiment, we change the distribution of inputs from normal to uniform, selecting as minimum and maximum values ± two standard deviations of the corresponding normal distributions.

From Figure 4, one can observe that simple random sampling results in noisier estimates and that this noise increases substantially the smaller the sample. Full factorial design sampling results in deterministic estimates for sensitivity indices, but the SBA performed on such a sample underestimates first-order indices and overestimates second-order effects. Quasi-Monte Carlo (QMC), done with scrambling, gives more accurate and clear estimates than other sampling strategies, even with a smaller sample, and, thus, is recommended for sensitivity indices computation. QMC is easy to implement and its coded functions are available in Julia (Robbe, 2018), Matlab (Math Works, 2013), Python (SciPy, 2023), and R (Chalabi et al., 2023). However, when using any of these packages, it is important to have the first point in the sequence sampled for uniformly distributed inputs, otherwise, its performance drops (Owen, 2020).

3.2. Capturing Cyclic Behaviour – The Ishigami Function

The Ishigami function, Equation (9), is one of the benchmark functions often used in sensitivity analysis studies for the validation of different methods, since analytical solutions for its sensitivity indices can be readily determined:
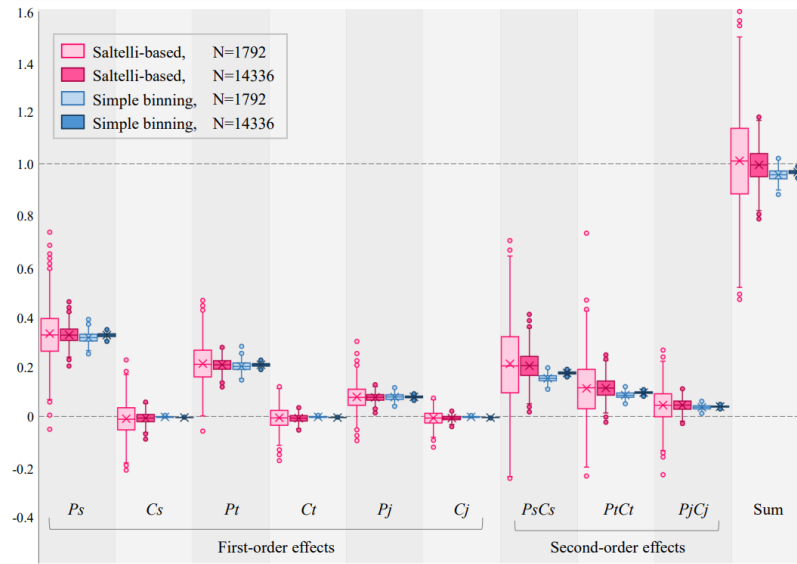
Figure 3. Sobol' indices for the portfolio model obtained with the Saltelli implementation (Saltelli, 2002) based on simple random sampling of sizes N = 128 × (2 × 6 + 2) = 1,792 and N = 1,024 × (2 × 6 + 2) = 14,336, and corresponding indices obtained with the SBA.
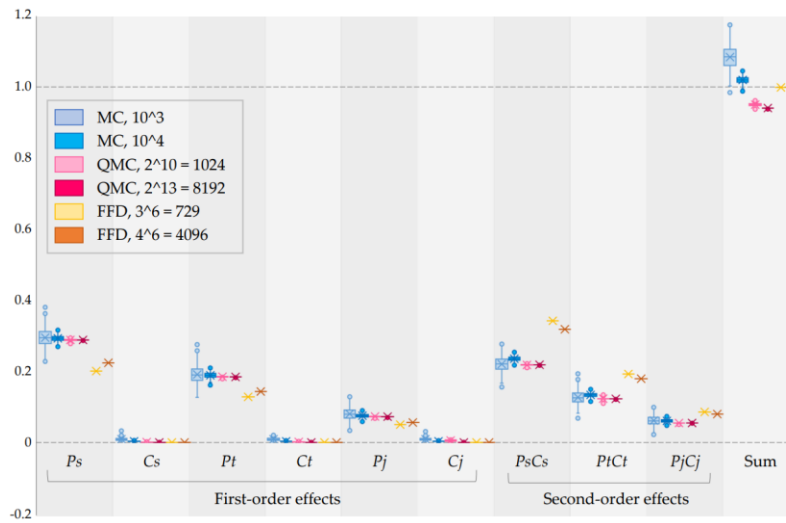

Figure 4. Portfolio model sensitivity indices estimation by the SBA with simple random sampling or Monte Carlo simulation (MC), quasi-random sampling or quasi-Monte Carlo (QMC), and full factorial design (FFD) sampling. The sample size is determined by the specifics of sampling techniques.
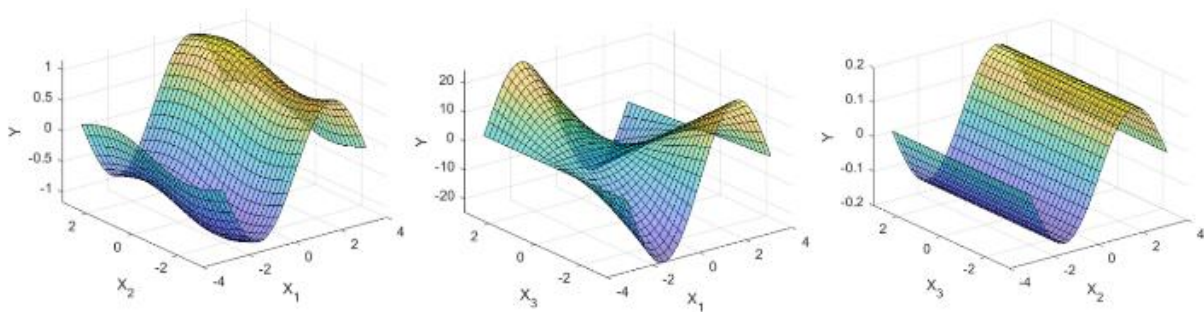

Figure 5. Ishigami function, Equation (9), with a = 7 and b = 0.1 (the third factor is fixed at 0 on each plot).

$$Y = \sin(X_1) + \alpha \sin(X_2)^2 + bX_3^4 \sin(X_1) \qquad (9)$$

The function is periodic in nature, Figure 5, which represents a significant challenge for approximate methods (Ziehn and Tomlin, 2009).

The SBA is tested on the Ishigami function with parameters $a = 7$ and $b = 0.1$, quasi-random sampling of different sample sizes, Figure 6.

Figure 6 indicates that the SBA with QMC sample size 2^{13} or larger captures first-order effects very well but underestimates the highly curved (see Figure 5 (center)) interaction effect between X_1 and X_3. A smaller sample translates into fewer bins for estimating the first-order effects and the square root of that for second-order effects (a sample size of 2^{10} is analyzed with 10 bins for first-order effects and only 3 bins for the second-order effects), so the high-frequency relationships are downplayed. Thus, if a model is known to possess periodic or cyclic effects, a larger sample size becomes essential in order to produce reliable estimates for sensitivity analysis.
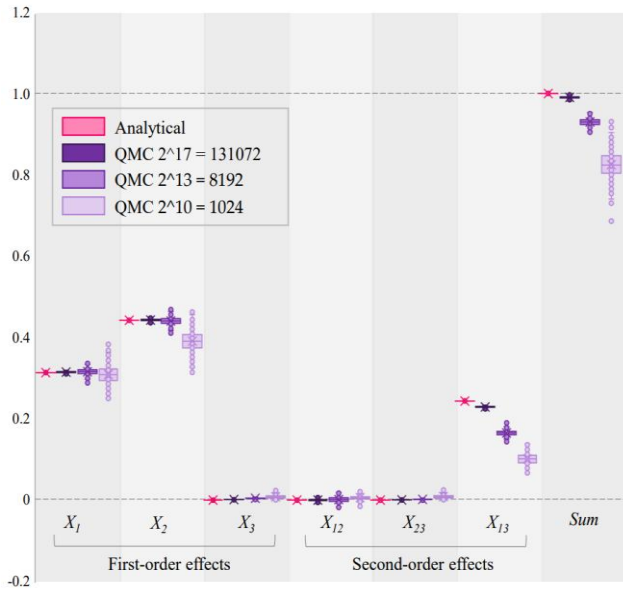

Figure 6. Analytical and approximate sensitivity indices for Ishigami function.

3.3. Capturing Correlation – The Mechanical Engineering Model

In this section, we reproduce and then modify the mechanical engineering problem presented in Marzban and Lahmer (2016) by introducing dependent inputs into their model and examining the resulting performance capabilities of our sensitivety analysis algorithm in processing this additional complication.

3.3.1. Case Background

Civil engineering structures play an essential role in most modern infrastructures (e.g., in buildings, process industry, and shells). A wide spectrum of steel frames is required within these structures. From an engineering perspective, such frames must be designed to withstand numerous different kinds of load actions due to such things as payloads, self-weight, and environmental impacts. In statically loaded structures (characterized by permanent load actions), it is necessary to analyze stresses and displacements. Stress analyses are usually related to the ultimate limit state (ULS), while analyses on displacement cover the serviceability limit states (SLS) that are affiliated with the operational conditions and functionalities (service) of structures. It is crucial to understand the effects of different parameters on the mechanical system's behaviour. For some simple cases, the effects can be determined analytically.

Frequently, however, nonlinear becomes impractical or impossible to solve analytically in even the most straightforward systems. In such cases, numerical modeling becomes a requisite tool for assessing structural behaviour under mechanical loads. From an engineering viewpoint, it is usually easy to determine the most influential geometric and material parameters in the underlying linear analyses (LAs) of mechanical behaviour of the system, such as deflections and stresses. However, geometrically nonlinear analyses (GNAs) may uncover different behaviour of the system with a different set of influential parameters. Thus, the decision, which analysis to use is often critical for engineering design and structural analysis.

To support the decision as to whether a nonlinear approach is required, a simplified model that computes the ratio between the results of two different analysis types (e.g., LA and GNA) can be employed. The sensitivity indices for different parameters can then provide insight for decision-making.

A two-dimensional frame structure is employed to demonstrate such an approach (Figure 7), as in (Marzban and Lahmer, 2016). The frame structure is comprised of two vertical columns joined with a horizontal beam. The beam is loaded by a uniformly distributed shear load along the beam and the top left corner of the frame is loaded by a horizontal load. The structural behaviour, focusing on the displacements, of the frame structure is numerically solved via LA and GNA.
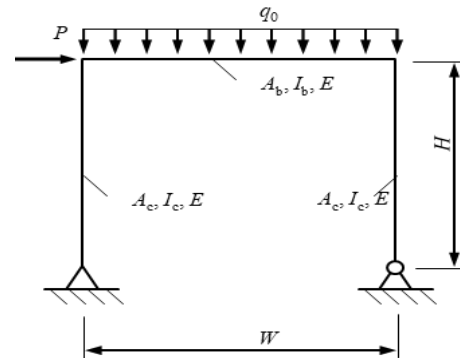

Figure 7. Shape and dimensions of the studied frame structure.

As the original CALFEM finite element (FE) code (Austrell et al., 2004) applied in Marzban and Lahmer (2016) was not accessible, a similar frame structure compiled by three beam elements was recreated (Figure 7). The numerical FE models

were parameterized in an API tool using the FEMAP 2022.2 (Siemens PLM) software. The system was studied employing nine different input parameters. Namely, the height H and width W of the frame; the modulus of elasticity E; the cross-sectional area of columns and beam, A_c and A_b, respectively; the second moment of areas of columns and beam, I_c and I_b, respectively; lateral force, P; and uniformly distributed shear load q_0. Each parameter was varied by $\pm 25\%$ of its mean value and Table 3 displays all of the corresponding minimum and maximum values. A total number of 10,000 models were simulated and analyzed using both LAs and GNAs. As an output value, the ratio between lateral displacements in the top left corner of the frame, obtained using GNA and LA, was used.

3.3.2. Estimation of Sensitivity Indices

Table 4 displays the first- and second-order sensitivity indices computed for the original model used in Marzban and Lahmer (2016). To clarify the visual perception, all index values less than 2% have been grayed out. As can be seen from Table 4, the frame height is the mode influencing parameter. The relative magnitudes shown for the first-order effects coincide with the those obtained by Marzban and Lahmer (2016).

The negligible second-order indices signify an absence of any interaction effects.

To introduce dependency into the system, the H/I_c ratio was fixed as per the dimensions of the case structure (i.e., $I_c = 4.706e - 6 \times H$). With this change in effect, to investigate the second-order effects of input parameters with correlated input parameters, a subsequent computational experiment was conducted with a total of 10,000 simulations. The new sensitivity indices calculated for this correlated system are presented in Table 5.

Comparing Tables 4 and 5, we can clearly observe the striking difference arising in the second-order effects. While for the original model, all second-order effects were negligible, in the correlated model, we can see a negative effect of 20%. The negative second-order effect reflects the introduced dependency between the inputs. It should be noted that this negative second-order effect essentially zeroes out the first-order effect of the I_c if summing up all effects. Thus, the negative second-order effect represents a correction of an overlapping first-order effect.

It can be further observed that the first-order indices have changed their values as well. By effectively eliminating one in-

Table 3. Model Parameter Ranges in the Frame Model

	H (m)	W (m)	E (GPA)	A_c (e-5 m^2)	I_c (e-5 m^4)	A_b (e-3 m^2)	I_b (e-5 m^4)	P (kN)	q_0 (kN/m)
Minimum	2.55	3.0	150	1.5	1.2	4.5	4.05	7.5	37.5
Maximum	4.25	5.0	250	2.5	2.0	7.5	6.75	12.5	62.5

Table 4. Sensitivity Indices for the Engineering Model

Input variables	H	W	E	A_c	I_c	A_b	I_b	P	q_0
First-order indices	41%	16%	13%	0%	10%	0%	0%	0%	13%
Second-order indices									
H		1%	1%	0%	0%	0%	0%	0%	1%
W			0%	0%	0%	0%	0%	0%	0%
E				0%	0%	0%	0%	0%	0%
A_c					0%	0%	0%	0%	0%
I_c						0%	0%	0%	0%
A_b							0%	0%	0%
I_b								0%	0%
P									0%

Table 5. Sensitivity Indices for the Modified Engineering Model with Correlated Inputs

Input variables	H	W	E	A_c	I_c	A_b	I_b	P	q_0
First-order indices	21%	27%	23%	0%	21%	0%	1%	0%	22%
Second-order indices									
H		1%	0%	0%	−20%	0%	0%	0%	2%
W			0%	0%	1%	0%	0%	0%	0%
E				0%	0%	0%	0%	0%	0%
A_c					0%	0%	0%	0%	0%
I_c						0%	0%	0%	2%
A_b							0%	0%	0%
I_b								0%	0%
P									0%

put variable via correlation, the overall output variance of the output has changed so that corresponding portions of the explained variance have also changed accordingly.

This engineering case demonstrates that the binning approach for calculating sensitivity indices is capable of capturing and identifying the impacts from dependent inputs.

Even though such sensitivity analyses can be time-consuming for complex systems (e.g., for a high number of elements), this approach could be used for sub-models to highlight the influencing factors and importance of GNAs. While in the presented example, the correlation was introduced artificially, it occurs naturally in more complex systems (e.g., strength properties are dependent on the material chosen, or, if giving an example outside engineering applications, different price ranges lead to different demand levels, etc.). Projecting these findings to a larger scope of applications, an increase in the accuracy of structural analyses for SLS estimates would improve the overall reliability and integrity of the structures. Consequently, costly required changes to structural elements potentially found post hoc during service/operation could be avoided via proper priori engineering analysis and design.

3.4. Dataset Size

For a sensitivity analysis study, it is important to know how many uncertain variables the method can process and how many simulation runs are needed to compute the indices to a certain level of precision. While the previous experiments (Figure 3 and Figure 6) provide a sense of index estimate precision as a function of the simulation runs, they do not factor in the number of uncertain variables – which is a crucial consideration, especially for computationally heavy models.

A straightforward pairwise multiplicative model is chosen to illustrate and evaluate how the precision of sensitivity indices estimates depends on the number of variables in the model and the number of simulation runs, because the analytical sum of all of its first- and second-order indices equals 1:

$$Y = \sum_{i=1}^{K_{factors}/2} X_i \times Z_i, \qquad (10)$$

where $K_{factors} \in \{2, 4, 10, 20, 50, 100, 200, 300\}$.

For $K_{factors} = 2$, the result of the model would simply be a multiplication of two variables $Y = X \times Z$. However, the numeric experiments will test up to 300 variables in the model. Both X and Z are assumed to be uniformly distributed in the range from 0 to 1 and sampled via simple random sampling. A simple random sampling scheme ensures worst-case accuracy results, which can then be used to derive the minimum number of simulation runs needed irrespective of the actual sampling strategy. As was demonstrated above, adopting QMC instead of simple random sampling would either institute substantial improvements in accuracy or, alternatively, reduce the number of simulation runs while preserving the same level of accuracy.

Since displaying box plots for all 300 variables would be unrealistic, the average errors that the SBA produces for each combination of the number of variables, $K_{factors}$, and the number of simulation runs $N_{runs} \in \{100, 250, 500, 750, 10^3, 5 \times 10^3, 10^4, 10^5, 10^6\}$ are determined, instead. The Mean Absolute Error (MAE) has traditionally been considered the "industry standard" test measure in sensitivity analysis studies (Saltelli et al., 2010). Consequently, the MAE can be calculated as:

$$MAE = \frac{1}{N_{rep}} \sum_{j=1}^{N_{rep}} \left| S_{esimated_j} \times S_{analytical} \right| \qquad (11)$$

where N_{rep} is the number of repetitions of the experiment for each combination of $K_{factors}$ and N_{runs}, and $S_{esimated_j}$ is the sum of the first- and second-order indices obtained in each experiment.

The experiments were undertaken in Matlab on the Puhti supercomputer using the following algorithm for each combination of $K_{factors}$ and N_{runs}:

(1) Compute the output Y of the model N_{runs} times and generate an input-output dataset of the size (N_{runs}, $K_{factors}$).

(2) Compute the first-order indices for all variables $K_{factors}$ and the second-order indices for each pair of variables and their sum $S_{esimated_j}$.

(3) Compute the error term for the sum of the indices as an absolute deviation of the sum of indices from its analytical value equal to 1.

(4) Repeat steps (1) ~ (3) 16 times (by running parallel computations on 8 cores, 2 times) and compute the *MAE* as the average of the errors computed in step (iii).

Table 6. MAE of The Sum of Sensitivity Indices for Different

| Number of variables, $K_{factors}$	Number of simulations, N_{runs}								
	100	250	500	750	10^3	5×10^3	10^4	10^5	10^6
2	0.16	0.12	0.05	0.03	0.02	0.00	0.00	0.00	0.00
4	0.49	0.18	0.07	0.05	0.03	0.03	0.01	0.01	0.01
10	3.94	1.59	0.78	0.50	0.37	0.05	0.01	0.04	0.04
20	16.84	6.83	3.40	2.23	1.64	0.32	0.15	0.01	0.01
50	110.32	44.17	21.93	14.63	10.95	2.16	1.07	0.08	0.02
100	445.49	177.62	88.99	59.22	44.56	8.87	4.44	0.42	0.02
200	1790.44	715.29	357.80	238.84	178.97	35.78	17.90	1.76	0.15
300	4031.79	1613.73	806.67	538.11	403.33	80.63	40.33	4.01	0.38
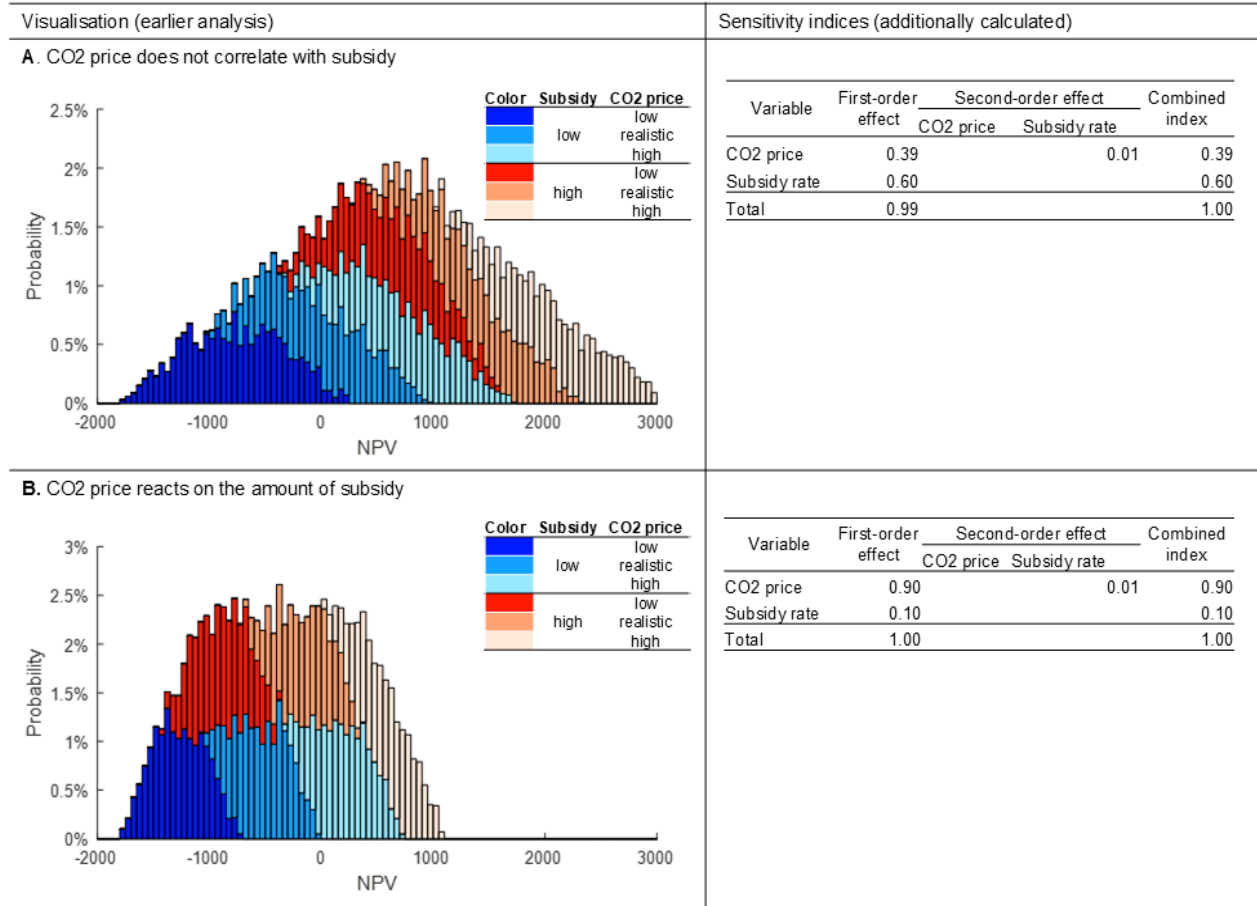
Figure 8. Supplementing the visual analytics from Kozlova & Yeomans (2019) (charts on left) with sensitivity indices (tables on right) for the two profitability possibilities of the carbon capture and storage investment.

The results from these experiments are presented in Table 6. Values below 0.05 correspond to high accuracy estimates and are displayed in green. Conversely, values exceeding 1 imply poor accuracy and are coloured red. Intermediate values between these limits have been colour-coded according to a relative, gradient-shaded basis.

Table 6 indicates that models possessing small numbers of variables do not require many simulation runs, even when using simple random sampling. For example, 500 runs would be more than sufficient to generate reasonably accurate estimates for models containing up to 4 variables. Ten thousand simulation runs would enable an increase to the number of variables to 10 without any perceived loss of accuracy, while one hundred thousand simulations would enable an increase of the number of variables to 20. One million simulation runs would be sufficient to produce accurate sensitivity indices estimates for models containing 100 variables. Models containing a larger number of variables would require more simulation runs.

While these results can be used to provide recommendations for the simulation size of different models with respect to establishing precision accuracy for their indices, less precise indices can also be used to provide meaningful information about the relative importance of different variables. Duly noting that the biggest source of numeric noise arises from second-order indices, when simulation resources are restricted in computationally intensive models, estimating only the first-order indices would still generate meaningful results. For example, Pellegrino et al. (2024) computed the first-order indices for their 30-variable model from only 1,000 simulation runs in order to efficiently pinpoint the most influential variables. Similarly, Pérez et al. (2024) created meaningful sensitivity indices using a subset of 152 data points to analyze the influences of 4 variables in their model. In both cases, the numeric estimates were validated with subsequent visualizations that confirmed the relative importance of the identified variables. Consequently, less accurate, but meaningful, sensitivity estimates of higher-dimensional models can be determined by using smaller simulation runs than those shown in Table 6 and the impacts of these estimates can be subsequently corroborated through appropriate SimDec visualizations.

3.5. Supplementing Visual Analytics with Sensitivity Indices – Carbon Capture Subsidy Model

Often the results of model simulation are studied qualita-

tively with various types of visualizations, such as classic histograms, heatmaps, and scatterplots. In this section, we demonstrate that supplementing visual analysis with the quantitative sensitivity indices computation provides additional validation for the conclusions.

Kozlova and Yeomans (2019) previously analyzed a carbon capture and storage subsidy model using the first-generation, visual-only version of the SimDec algorithm. The rationale behind the model is to evaluate the profitability of a carbon capture investment under a subsidy, contrasting the two possibilities – (i) with and (ii) without a reaction of the price of the CO_2 to the subsidy levels. The straightforward model only considers two uncertain input variables, the *CO_2 price* varying between 0 and 50 \$/t, and the *subsidy* varying between 0 and 0.05 \$/kWh, both uniformly distributed. Figure 8 illustrates the reproduced simulation analysis based on the original model of Kozlova and Yeomans (2019) supplemented by the values calculated for the newly created sensitivity indices generated via the SBA approach.

The charts showing the decomposition performed using the *subsidy* and *CO_2 price* variables highlight the pronounced effect of both variables on the overall project profitability (*NPV*). The computed indices support the conclusion revealing a 60% combined effect from the *subsidy* and the remaining 39% influence attributable to the *CO_2 price* (Figure 8(A)). Note that the second-ord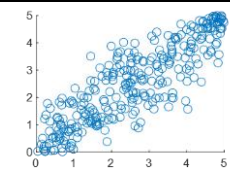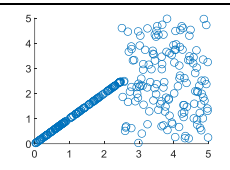er effects are negligible. The same originally randomized inputs are taken into further calculation, where a *CO_2 price* drop is modeled as a function of the *subsidy* level and the number of coal plants receiving it, modeling the possible dependency between the two. The decomposition reflects the changes, where the amount of subsidies no longer influences *NPV* to the same extent (low/blue and high/orange levels of subsidies have largely overlapping sub-distributions), but the original levels of *CO_2 price* still produce considerable shift in *NPV* (Figure 8(B)). This visualization conclusion is analytically reinforced and strongly supported by the values determined for the sensitivity indices. Computed indices demonstrate that while the combined effect of *subsidy* drops to only 10% from 60%, the *CO_2 price* becomes the more influential effect with a sensitivity index that rises to 90% from 40%. Once again, the second-order effects remain inconsequential.

4. Further Exploring the Relationships Between Second-Order Indices and Correlation

The mechanical engineering model demonstrated that the second-order sensitivity index turns negative in the presence of positive correlation (Table 5). But how does the index behave when the correlation is negative? Furthermore, is the relationship the same in the presence of an interaction of inputs that affect the output?

To explore these questions, we set up a series of simulation

Table 7. Sensitivity Indices and Correlation Coefficients for A Simple Y = AB Model with A and B Dependent to Different Degrees

Correlation Type	Model	S	Correlation								
			Negative				Positive				
			−100%	…	−50%	…	0%	…	50%	…	100%
	A + B	S_A		0.14	0.27	0.38	0.50	0.62	0.74	0.87	1.00
		S_B		0.14	0.27	0.38	0.50	0.62	0.74	0.87	1.00
		S_{AB}		0.71	0.47	0.23	0	−0.24	−0.49	−0.74	−1.00
		Σ		1.00	1.00	1.00	1.00	1.00	1.00	1.00	1.00
	AB	S_A	1.00	0.31	0.27	0.33	0.43	0.56	0.70	0.85	1.00
		S_B	1.00	0.31	0.27	0.33	0.43	0.56	0.70	0.85	1.00
		S_{AB}	−1.00	0.39	0.47	0.35	0.14	−0.11	−0.40	−0.70	−1.00
		Σ	1.00	1.00	1.00	1.00	1.00	1.00	1.00	1.00	1.00
	Pearson		−1.00	−0.73	−0.48	−0.24	0	0.24	0.48	0.73	1.00
	Spearman		−1.00	−0.73	−0.48	−0.24	0	0.24	0.48	0.73	1.00
	A + B	S_A		0.61	0.36	0.45	0.05	0.65	0.79	0.93	1.00
		S_B		0.04	0.23	0.47	0.05	0.67	0.76	0.83	1.00
		S_{AB}		0.35	0.39	0.09	0	−0.32	−0.56	−0.76	−1.00
		Σ	1.00	1.00	1.00	1.00	1.00	1.00	1.00	1.00	1.00
	AB	S_A	1.00	0.52	0.39	0.42	0.43	0.44	0.51	0.74	1.00
		S_B	1.00	0.09	0.17	0.35	0.43	0.59	0.86	0.93	1.00
		S_{AB}	−1.00	0.39	0.44	0.24	0.14	−0.03	−0.36	−0.67	−1.00
		Σ	1.00	1.00	1.00	1.00	1.00	1.00	1.00	1.00	1.00
	Pearson		−1	−0.71	−0.52	−0.23	0	0.23	0.52	0.71	1.00
	Spearman		−1	−0.71	−0.53	−0.24	0	0.24	0.53	0.71	1.00

experiments for two simple two-factor models. The first model is additive, $Y = A + B$, where the variables do not interact. The second model is multiplicative, $Y = AB$, which possesses a positive second-order effect when the variables are independent, thereby manifesting interaction. We also examine two different types of correlation, (i) joint multivariate uniform distribution copula and (ii) equating values of B to A over a portion of the sample, which might be considered as a structural change in the system. Both correlation types are modeled for different correlation strengths. For validation purposes, Pearson and Spearman correlation coefficients are reported in each case. Both A and B assume uniform distribution between 0 and 5. The indices are calculated based on a sample size of 106 to ensure a high level of precision.

The sensitivity indices estimates are presented in Table 7, and the relationship between the second-order indices and the Pearson correlation coefficient is visualized in Figure 9. Hart and Gremaud (2018) and Idrissi et al. (2023) have indicated that theoretical second-order indices can become negative in the presence of dependent inputs and such an outcome can be observed for the approximated indices computed by the SBA (Table 7).
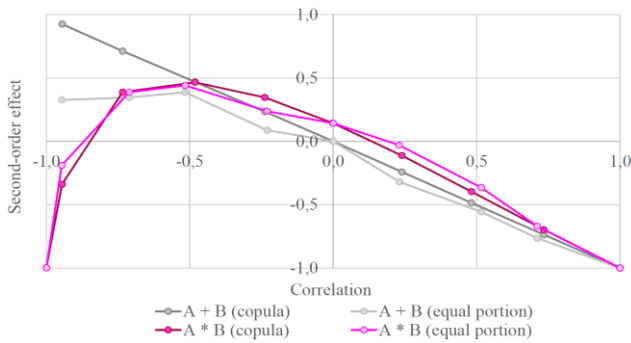

Figure 9. Second-order effect as a function of correlation for additive (0% interaction) and multiplicative (14% interaction) functions with two correlation types, (1) portion of equal values, (2) copula.

Additive models cross the origin (see Figure 9) and possess zero second-order effects under a no-dependency case. No interaction is anticipated from the additive model. Copula variables show the second-order effect values very close to the correlation coefficients and form a linear relationship between the two. Positive correlation results in negative second-order effects, conveying overlapping effects of the variables. Conversely, negative correlation results in a positive second-order effect for additive models as if the combined effect of the variables is greater than the sum of their individual effects (see Equation (5)).

The additive model, in which dependence is modeled through a portion of equal values, has largely the same pattern except for lower positive second-order effects in the presence of negative correlation. The calculation of significance indices for both additive models at −100% correlation fails, because all Y values turn to 0. Instead, the values for the negative 95% correlation

are computed and displayed in Figure 9.

In the multiplicative model, the second-order effect index behaves asymmetrically for positive and negative correlation (Figure 9). With increasing positive correlation, the second-order index becomes increasingly negative (as in the additive models), signifying the overlapping effects of the input variables on the output. For negative correlations, the second-order index is initially positive and increasing, peaking at 50% correlation. This translates into a synergistic effect where the negatively correlated inputs magnify the impact on the output. But when the negative correlation exceeds 50%, the second-order index decreases and approaches −1. One could speculate that with a strong negative correlation for interacting variables, the joint overlapping effect becomes stronger than the synergistic one, driving the second-order index to −1.

For all cases, the conservation property (the sum of all indices is equal to 1) holds. The boundedness property for each index extends from [0, 1], as for the classic Sobol' indices, to [−1, 1]. Because the conservation property holds under all cases, this implies that correlation and interaction effects are actually both combined into the single second-order effect, and simultaneously affecting the first-order index behaviour, perfectly fitting into the variance decomposition of the output. The presence of interaction can be observed in Figure 9 as the vertical distance between the additive and multiplicative models' lines on the correlation range between −0.25 and 0.25. In other words, the different degrees of dependency move the second-order effect up or down, but the presence of interaction reveals itself in higher second-order effect values. These findings correspond with the recent breakthrough in the theory of sensitivity analysis, which suggests that the second-order effect can be considered as a projection of a strength of interaction conditioned by the strength of the dependency between the input variables (Idrissi et al., 2023).

5. Visualizing Second-Order Effects – Beyond Sensitivity Indices

The sensitivity analysis field has focused on computing sensitivity indices to be able to rank the input variables by their relative importance (Saltelli et al., 2008; Da Veiga et al., 2021). And yet it becomes apparent that sensitivity indices are not able to convey the full relationship story. As observed in our earlier analysis with dependent input variables (Table 7), the second-order indices for the same model, but operating under different assumptions, appear to be very similar. However, the scatter plots (Table 7) reveal how different these relationships actually are, and this knowledge can lead to different structural design decisions.

A fact that has been largely neglected throughout modern sensitivity analysis studies is that although specific summary values can appear near-identical in magnitude, an examination of the underlying data can reveal very different shapes and perspectives (Saltelli et al., 2004; Puy et al., 2022; Kozlova et al., 2024a).

Consequently, different kinds of visualizations can be used

to augment and improve the understanding of the underlying model. These data visualizations can include such formats as basic scatter plots, response surfaces, heat maps, and parallel coordinate plots. However, all of these representations possess dimensionality limitations. SimDec is a recent approach that is able to project multidimensional systems onto a two-dimensional graph (Kozlova and Yeomans, 2022b) and, in combination with the SBA for global sensitivity analysis, can be used to convey the nature of interactions in complex models to produce a much more comprehensive sensitivity analysis framework (Kozlova et al., 2024a).

To illustrate the power of this framework, this section showcases the application of the SBA together with SimDec visualization for investigating the behaviour of a complex structural reliability model containing both correlations and interactions.

5.1. Case Background: Structural Reliability Model for Fatigue Assessments

Many structural applications experience cyclic or fluctuating load conditions during service life (such as ship and offshore structures as well as various vehicles, trucks and trains). In these complex systems, fatigue is amongst the most important design criteria to control and maintain the lifespan of ageing components without concerns of structural failures. Due to the random nature of acting cyclic loads in many applications and the complexity of physical modeling of fatigue phenomenon, the vast majority of existing models for predicting fatigue life are necessarily based on probabilistic or data-driven approaches (Leonetti et al., 2020; Ruiz Muñoz and Sorensen, 2020; Bai et al., 2023; Ye et al., 2023). However, current trends for improving material usage and optimization in mechanical components have led to an ever-increasing need for creating more sophisticated and more accurate deterministic models to assess the fatigue life of components. This is particularly the case for modern infrastructures that utilize high-strength steels, due to the fact that an increase in material strength does not contribute to higher fatigue performance in welded components (Lieurade et al., 2008).

To account for the effects of material strength and welding quality, a multi-parametric model–named the 4R method–was introduced for fatigue assessment of welded components. The 4R model incorporates four parameters–material strength, welding residual stresses, applied stress ratio, and welding quality (Ahola et al., 2020; Ahola et al., 2021; Ahola et al., 2024).

These four key parameters affect the fatigue strength of welded components depending on the conditions (Hobbacher, 2016). As the 4R model employs more parameters than conventional models, a key question still rests on a determination of the sensitivity of each parameter on the 4R output value.

The basis of the 4R method is to utilize the effective stress concept, usually known as the effective notch stress (ENS) approach (Sonsino et al., 2012), in association with the mean stress correction using the requisite four parameters. In the 4R model, material elastic-plastic behaviour at the notch root is analytically or numerically computed, after which the local hysteresis loops of cyclic stress are determined. The output reference stress applied in fatigue assessments (in the form of S-N curve) is computed based on the well-known Smith-Watson-Topper (Smith et al., 1970) mean stress correction on the linear-elastic notch stress (Equation (12)). Figure 10 demonstrates the workflow of the 4R method.

$$\Delta\sigma_{k,ref} = \frac{\Delta\sigma_k}{\sqrt{1 - R_{local}}} \tag{12}$$

5.2. Sensitivity Indices for the Structural Reliability Model

The 4R model is simulated 104 times with inputs uniformly distributed within the ranges specified in Table 8. The three levels of residual stress and stress ratio for each case material are formed based on actual conditions in structural components. Usually welding causes high tensile residual stresses, up to the yield strength of parent material. On the other hand, residual stresses can be reduced by, for example, postheat treatments and/or mechanical post-weld treatments or residual stress relaxation via the mechanical load. The applied stress ratio is specific to load conditions in service, and the selected three cases represent available cases in engineering components. The weld toe radius is converted in the model to fatigue-effective stress, K_f, the sensitivity to which is analyzed. The three other inputs used in the sensitivity analysis, as is. The sensitivity indices to the model output, $\Delta\sigma_{k,ref}$, computed with the SBA, are presented in Table 9.

The sensitivity indices in Table 9 show that the residual stress σ_{res}, alone, explains half of the variance of the output. Residual stress σ_{res} also has 11% interaction with stress ratio R, and a negative −6% second-order effect with steel grade $R_{p0.2}$. In addition, stress ratio R and steel grade $R_{p0.2}$ have a 4% inter-
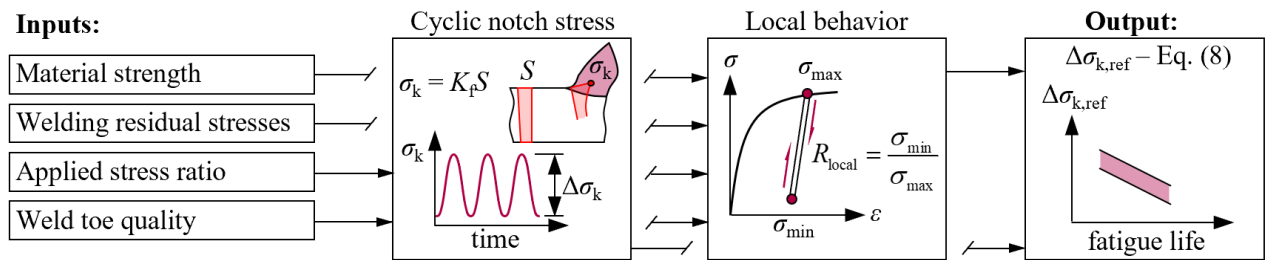

Figure 10. Description and workflow of the 4R model for fatigue assessment.

Table 8. Assumptions on Input Variation for the Structural Reliability 4R Model

Case material	r_{ture} (mm)	$R_{p0.2}$ (MPa)	σ_{res} (MPa)	R (-)
S355	0.5 ± 0.5	355 ± 100	250 ± 100	0.5 ± 0.2
			0 ± 100	0 ± 0.2
			-100 ± 100	-1 ± 0.2
S960	0.5 ± 0.5	960 ± 100	850 ± 100	0.5 ± 0.2
			0 ± 100	0 ± 0.2
			-300 ± 100	-1 ± 0.2

Table 9. Sensitivity Indices for the Structural Reliability 4R Model

Variable	First-order effect	Second-order effect				Combined effect
		Residual stress, σ_{res}	Stress ratio, R	Steel grade, $R_{p0.2}$	Fatigue-effective stress, K_f	
Residual stress, σ_{res}	50%		11%	-6%	0%	51%
Stress ratio, R	28%			4%	0%	35%
Steel grade, $R_{p0.2}$	11%				0%	10%
Fatigue-effective stress, K_f	4%					4%
Σ	92%					100%

action. The remaining second-order effects are zero. Thus, there are three input variables in the model that have pairwise interaction effects with each other: residual stress σ_{res}, stress ratio R, and steel grade $R_{p0.2}$. Together these variables explain 96% of the output variability. However, as mentioned above, the sensitivity indices alone cannot adequately explain the nature of those interactions and how they should be accounted for in decision-making processes.

5.3. Exploring the Nature of Second-Order Effects

To investigate how the model output is affected simultaneously by the three input variables identified as possessing pairwise interaction effects, we employ SimDec to provide a multi-dimensional visualization perspective of their impacts (Kozlova et al., 2022a; Kozlova and Yeomans, 2024a). Since SimDec uses a frequency distribution, the same simulation data that was used to compute sensitivity indices with the simple binning method, can be used for the visualization. The idea behind SimDec is to decompose the simulation data into regions formed by the combinations of different ranges (or states) of influential input variables. An intelligent colour-coding of these regions in the frequency distribution communicates a clear visual representation of the inherent input-output relationships within the model (for the algorithm details, see (Kozlova et al., 2024a). The open-source SimDec code is available for Python, R, Julia, and Matlab (Kozlova et al., 2023).

For the structural reliability model, we choose to break down the residual stress σ_{res} into three states (low, medium, high),

the stress ratio R into two states (reversed, pulsating), and the steel grade $R_{p0.2}$ into two states (mild, UHSS) (Table 10).

Altogether, all possible combinations of these state settings for the input variables (Table 10) form 12 separate scenarios. The probability distribution of the model output, $\Delta\sigma_{k,ref}$, is partitioned using these scenarios and colour-coded. The colouring logic is important to facilitate the overall interpretability of the visual perceptions. The states of the most influential input variable assume distinct main colours, and each of these main colours is sub-shaded to further highlight the partitions, Figure 11.

Figure 11 demonstrates how non-monotonic the effects of the input variables on the model output are, and that the effect of one input is conditioned to the states of another one. First, the residual stress σ_{res} divides the distribution into two narrow scenarios, medium and high, whereas the low scenario sub-distribution spreads out through the entire range of the output values. Stress ratio R has only a minor effect on the output in medium and high states of residual stress (small horizontal shift of the respective sub-distributions) but plays an important role in the low residual stress, almost dividing the output into halves. In low residual stress, steel grade $R_{p0.2}$ has a minor effect when the stress ratio is reversed but creates a substantial rightward shift if the stress ratio is pulsating. The combinations of medium residual stress and UHSS steel grade and high residual stress and mild steel grade are non-existent, which reflects physical material constraints and thereby explains the negative second-order effect. These visceral relationships would not have been revealed or apparent without the SimDec visualization.

Table 10. Decomposition Set-Up for The Structural Reliability 4R Model (UHSS Stands for Ultra-High Steel Strength)

Residual stress			Stress ratio			Steel grade		
State	min	max	State	min	max	State	min	max
Low	-400	100	Reversed	-1.20	-0.25	Mild	255	657
Medium	100	650	Pulsating	-0.25	0.7	UHSS	657	1,060
High	650	950						

Color	Scenario	Residual stress, σ_{res}	Stress ratio, R	Steel grade, $R_{p0.2}$	Output Summary			
					min	mean	max	probability
	sc1		Reversed	Mild	107	332	475	11%
	sc2		Reversed	UHSS	11	264	515	11%
	sc3	Low	Pulsating	Mild	320	467	591	22%
	sc4		Pulsating	UHSS	68	543	819	22%
	sc5		Reversed	Mild	383	456	524	6%
	sc6		Reversed	UHSS	NaN	NaN	NaN	NaN
	sc7	Medium	Pulsating	Mild	422	499	622	12%
	sc8		Pulsating	UHSS	NaN	NaN	NaN	NaN
	sc9		Reversed	Mild	NaN	NaN	NaN	NaN
	sc10		Reversed	UHSS	630	704	795	6%
	sc11	High	Pulsating	Mild	NaN	NaN	NaN	NaN
	sc12		Pulsating	UHSS	656	746	851	12%

Figure 11. Simulation decomposition of the structural reliability 4R model.

6. Conclusions

This paper introduces and extensively tests the SBA for computing first- and second-order sensitivity indices, which provide more accurate results than classic global sensitivity analysis measures for Sobol' indices.

The extensive experimentation revealed the following advantages for SBA in comparison to the mainstream estimator of Sobol' indices: (i) By requiring substantially fewer simulation runs, SBA is considerably more computationally efficient; (ii) In turn, this finding enables SBA to be applied to more complex models that possess a significantly larger number of variables and/or are more computationally expensive; (iii) SBA performs extremely well using simple random sampling, thereby, greatly simplifying the requisite simulation tasks of practitioners; (iv) SBA is able to operate with input variables that are dependent, where negative values calculated for the second-order indices reveal which variables are correlated; (v) Consequently, SBA can also work effectively with given (i.e. empirical) data

sets that have not been produced exclusively from the numerical simulations of models; (vi) SBA computes first- and second-order indices instead of first- and total-order effects. The sum of the SBA indices becomes an indicator of how much of the output variance is explained by the given inputs. The sum can be used to detect possibly missed variability in the model, if it deviates from 1; (vii) Understanding the process of the SBA algorithm is very straightforward and it is easy to demonstrate visually through a binned scatterplot.

The major disadvantage in operating the SBA is that it requires the setting of a parameter for the number of bins. However, this disadvantage is eliminated through an automated definition of the number of bins. As was shown in the computational experimentation, the automation process generated extremely high accuracy for the sensitivity indices in all datasets over the various numbers of variables and sizes of simulations.

In all cases considered, the SBA was capable of revealing underlying sensitivities within the models irrespective of their overriding complexity. Of particular note, the conservation property of SBA indices in the presence of dependent variables in-

15

troduces new levels of analytical sophistication into sensitivity analysis. Consequently, problem realism can be readily preserved by including dependent and/or correlated input variables in the models (Kozlova et al., 2024b). Even more notably, essential dependencies in the form of non-complete hypercubes (input spaces) resulting from physical system limitations (i.e. missing combinations of certain input variable value ranges) need no longer be treated as an obstacle when conducting sensitivity analyses. Furthermore, SBA enables the design of new types of studies in which various different levels of a model can be subjected to distinct types of sensitivity analysis. For example, Myers et al. (2024) and Vinitskaia et al. (2024) analyzed the influence of aggregate variables composed from multiple uncertain input variables, while Pérez et al. (2024) studied the interrelationships between several different model outputs. Finally, from the combined indices in the presence of dependent inputs, the conservation property creates a significant research approach for examining correlation-interaction within second-order effects. Exploring this avenue had earlier been identified as a topic of vital research importance in contemporary theoretical sensitivity analysis studies (Hart and Gremaud, 2018; Idrissi et al., 2023).

The visual analytics component of SimDec supersedes other visualization approaches (Kozlova et al., 2024b) and has already been tested on numerous cases in several different disciplines (Kozlova and Yeomans, 2024). SimDec could potentially become the visualization standard throughout global sensitivity analysis. Its key advantage is that it exposes the shape of the underlying multivariable relationships. Kozlova et al. (2024a) showed that these shapes can be very different for interaction relationships even though they might be characterized by very similar amplitudes when measured by their second-order effects. Furthermore, it was noted that SimDec visualizations can be used to validate sensitivity indices for those cases exceeding the accuracy frontier of SBA.

The automated SBA-SimDec procedure can be readily extended and adjusted to incorporate the benefits from other methods. Such adjustments could include the substituting of SBA with any other global sensitivity analysis technique, supplementing SimDec with other model validation techniques, uncertainty quantification approaches, or visualization methods. It could even involve expanding the analysis using any other specific analytical/valuation methods, such as using real options or computing value-at-risk for the different SimDec scenarios.

The resulting methodological framework is streamlined, open-sourced, and provides an intuitive way of 'looking' into a computational model and grasping its underlying behaviour. The paper has demonstrated the importance of visualizing input-output relationships on various application models using the SimDec approach. The framework presented can be recommended for analyzing disparate complex models from many different disciplines, including environmental science, engineering, and business in order to holistically support policy- and decision-making. The extension of these analytical avenues to a wider range of applications in the environmental domain will be explored more extensively in subsequent research.

References

Ahola, A., Skriko, T. and Björk, T. (2020). Fatigue strength assessment of ultra-high-strength steel fillet weld joints using 4R method. *Journal of Constructional Steel Research*, 167, 105861. https://doi.org/10.1016/j.jcsr.2019.105861

Ahola, A., Muikku, A., Braun, M. and Björk, T. (2021). Fatigue strength assessment of ground Fillet-Welded joints using 4R method. *International Journal of Fatigue*, 142, 105916. https://doi.org/10.1016/j.ijfatigue.2020.105916

Ahola, A., Kozlova, M. and Yeomans, J.S. (2024). Capturing multi-dimensional nonlinear behaviour of a steel structure reliability model-global sensitivity analysis. *Sensitivity Analysis for Business, Technology and Policymaking Made Easy with Simulation Decomposition (SimDec)*. Routledge Publishing, Abingdon, Oxford-shire, UK, pp 257-282. https://doi.org/10.4324/9781003453789-15

Alam, A., Kozlova, M., Leifsson, L. and Yeomans, J.S. (2023). The importance of intelligent colouring for simulation decomposition in environmental analysis. *Journal of Environmental Informatics Letters*, 10(2), 63-73. https://doi.org/10.3808/jeil.202300118

Alidoosti, A., Ghafari-Nazari, A., Moztarzadeh, F., Jalali, N., Moztarzadeh, S. and Mozafari, M. (2013). Electrical discharge machining characteristics of Nickel-Titanium shape memory alloy based on full factorial design. *Journal of Intelligent Material systems and Structures*, 24(13), 1546-1556. https://doi.org/10.1177/1045389X13476147

Austrell, P.E., Dahlbom, O., Lindemann, J., Olsson, A., Olsson, K.G., Persson, K., Petersson, H., Ristinmaa, M., Sandberg, G. and Wernberg, P.M. (2004). *CALFEM - A finite element Toolbox, version 3.4*. Studentlitteratur AB. ISBN: 9789188558237

Bai, S., Huang, T., Li, Y.F., Lu, N. and Huang, H.Z. (2023). A probabilistic fatigue life prediction method under random combined high and low cycle fatigue load history. *Reliability Engineering & System Safety*, 238, 109452. https://doi.org/10.1016/j.ress.2023.109452

Barr, J. and Rabitz, H. (2023). Kernel-based global sensitivity analysis obtained from a single data set. *Reliability Engineering & System Safety*, 235, 109173. https://doi.org/10.1016/j.ress.2023.109173

Borgonovo, E. (2007). A new uncertainty importance measure. *Reliability Engineering & System Safety*, 92(6), 771-784. https://doi.org/10.1016/j.ress.2006.04.015

Borgonovo, E., Plischke, E. and Prieur, C. (2024). Total effects with constrained features. *Statistics and Computing,* 34, 87. https://doi.org/10.1007/s11222-024-10398-5

Caers, J. 04-2 Sensitivity Analysis Global. Lecture, Stanford University course "QUSS GS 260". https://youtu.be/vBuWB9WuFhA (accessed October 1, 2018)

Chalabi, Y., Dutang, C., Savicky, P., Wuertz, D., Knuth, D., Matsumoto, M. and Saito, M. (2023). *Toolbox for Pseudo and Quasi Random Number Generation and Random Generator Tests*. https://cran.r-project.org/web/packages/randtoolbox/randtoolbox.pdf

Crestaux, T., Le Maître, O. and Martinez, J.M. (2009). Polynomial chaos expansion for sensitivity analysis. *Reliability Engineering & System Safety*, 94(7), 1161-1172. https://doi.org/10.1016/j.ress.2008.10.008

Cukier, R., Fortuin, C., Shuler, K.E., Petschek, A. and Schaibly, J.H. (1973). Study of the sensitivity of coupled reaction systems to un-

certainties in rate coefficients. I Theory. *The Journal of Chemical Physics*, 59(8), 3873-3878. https://doi.org/10.1063/1.1680571

Da Veiga, S. (2015). Global sensitivity analysis with dependence measures. *Journal of Statistical Computation and Simulation*, 85(7), 1283-1305. https://doi.org/10.1080/00949655.2014.945932

Da Veiga, S., Gamboa, F., Iooss, B. and Prieur, C. (2021). *Basics and Trends in Sensitivity Analysis: Theory and Practice in R*. SIAM, pp 1-291. https://doi.org/10.1137/1.9781611976694

Deviatkin, I., Kozlova, M. and Yeomans, J.S. (2021). Simulation decomposition for environmental sustainability: Enhanced decision-making in carbon footprint analysis. *Socio-Economic Planning Sciences*, 75, 100837. https://doi.org/10.1016/j.seps.2020.100837

Di Maio, F., Gallo, N., Arcangeli, D., Taroni, M., Selva, J. and Zio, E. (2023). A bootstrapped modularised method of global sensitivity analysis applied to probabilistic seismic hazard assessment. *Structural Safety*, 101, 102312. https://doi.org/10.1016/j.strusafe.2022.102312

Ehre, M., Papaioannou, I. and Straub, D. (2024). Variance-based reliability sensitivity with dependent inputs using failure samples. *Structural Safety*, 106, 102396. https://doi.org/10.1016/j.strusafe.2023.102396

Hart, J. and Gremaud, P.A. (2018). An approximation theoretic perspective of Sobol' indices with dependent variables. *International Journal for Uncertainty Quantification*, 8(6). 483-493. https://doi.org/10.1615/Int.J.UncertaintyQuantification.2018026498

Hobbacher, A.F. (2016). *Recommendations for Fatigue Design of Welded Joints and Components*. Springer: Cham. pp 1-143. https://doi.org/1 0.1007/978-3-319-23757-2

Homma, T. and Saltelli, A. (1996). Importance measures in global sensitivity analysis of nonlinear models. *Reliability Engineering & System Safety*, 52(1), 1-17. https://doi.org/10.1016/0951-8320(96)00002-6

Idrissi, M.I., Bousquet, N., Gamboa, F., Iooss, B. and Loubes, J.M. (2023). Understanding black-box models with dependent inputs through a generalization of Hoeffding's decomposition. *arXiv pre-print*, arXiv: 2310.06567v3. https://doi.org/10.48550/arXiv.2310. 06567

Iooss, B., Sudret, B., Piano, L. and Prieur, C. (2022). Editorial for the special issue on "sensitivity analysis of model outputs". *Reliability Engineering & System Safety*, 223, 108477. https://doi.org/10.1016/j.ress.2022.108477

Jia, D.W. and Wu, Z.Y. (2024). An improved adaptive Kriging model for importance sampling reliability and reliability global sensitivity analysis. *Structural Safety*, 107, 102427. https://doi.org/10.1016/j.strusafe.2023.102427

Jung, W. and Taflanidis, A.A. (2023). Efficient global sensitivity analysis for high-dimensional outputs combining data-driven probability models and dimensionality reduction. *Reliability Engineering & System Safety*, 231, 108805. https://doi.org/10.1016/j.ress.2022.108805

Kozlova, M. and Yeomans, J. (2019). Multi-variable simulation decomposition in environmental planning: An application to carbon capture and storage. *Journal of Environmental Informatics Letters*, 1(1), 20-26. https://doi:10.3808/jeil.201900003

Kozlova, M. and Yeomans, J. (2020). Visual analytics in environmental decision-making: a comparison of overlay charts versus simulation decomposition. *Journal of Environmental Informatics Letters*, 4(2), 93-100. https://doi:10.3808/jeil.202000047

Kozlova, M. and Yeomans, J. (2022a). Extending simulation decomposition analysis into systemic risk planning for domino-like cascading effects in environmental systems. *Journal of Environmental Informatics Letters*, 7(2), 64-68. http://dx.doi.org/10.3808/jeil.202200079

Kozlova, M. and Yeomans, J.S. (2022b). Monte Carlo enhancement via simulation decomposition: a "must-have" inclusion for many disciplines. *INFORMS Transactions on Education*, 22(3), 147-159. https://doi.org/10.1287/ited.2019.0240

Kozlova, M., Roy, P., Moss, R.J. and Alam, A. *SimDec Repositories in Python, R, Julia, and Matlab*. https://github.com/Simulation-Decomposition (accessed October 1, 2023)

Kozlova, M., Moss, R.J., Yeomans, J.S. and Caers, J. (2024a). Uncovering heterogeneous effects in computational models for sustainable decision-making. *Environmental Modelling & Software*, 171, 105898. https://doi.org/10.1016/j.envsoft.2023.105898

Kozlova, M. and Yeomans, J.S. (2024). *Sensitivity Analysis for Business, Technology, and Policymaking Made Easy with Simulation Decomposition*. Routledge, pp 402. https://doi.org/10.4324/9781003453789

Kozlova, M., Lo Piano, S. and Yeomans, J.S. (2024b). Methodological landscape of sensitivity analysis and the place of SimDec. *Sensitivity Analysis for Business, Technology and Policymaking Made Easy with Simulation Decomposition (SimDec)*. Routledge, pp 3-26. https://doi.org/10.4324/9781003453789-2

Kozlova, M., Moss, R., Roy, P., Alam, A. and Yeomans, J.S. (2024c). SimDec algorithm and guidelines for its usage and interpretation. *Sensitivity Analysis for Business, Technology and Policymaking Made Easy with Simulation Decomposition (SimDec)*. Routledge, pp 27-59. https://doi.org/10.4324/9781003453789-3

Kucherenko, S., Albrecht, D. and Saltelli, A. (2015). Exploring multidimensional spaces: A comparison of Latin hypercube and Quasi-Monte Carlo sampling techniques. *arXiv preprint*, arXiv: 1505.02350. https://doi.org/10.48550/arXiv.1505.02350

Kucherenko, S. and Song, S. (2016). Derivative-based global sensitivity measures and their link with Sobol' sensitivity indices. *Monte Carlo and Quasi-Monte Carlo Methods: MCQMC, Springer Proceedings in Mathematics & Statistics*, Leuven, Belgium. https://doi.org/10.1007/978-3-319-33507-0_23

Kucherenko, S., Klymenko, O.V. and Shah, N. (2017). Sobol' indices for problems defined in Nonrectangular domains. *Reliability Engineering & System Safety*, 167, 218-231. https://doi.org/10.1016/j.ress.2017.06.001

Kucherenko, S. and Song, S. (2017). Different Numerical Estimators for Main Effect Global Sensitivity Indices. *Reliability Engineering & System Safety*, 165, 222-238. https://doi.org/10.1016/j.ress.2017.04.003

Lamboni, M. and Kucherenko, S. (2021). Multivariate sensitivity analysis and derivative-based global sensitivity measures with dependent variables. *Reliability Engineering & System Safety*, 212, 107519. https://doi.org/10.1016/j.ress.2021.107519

Leonetti, D., Majlaars, J. and Snijder, H.H. (2020). Probabilistic fatigue resistance model for steel welded details under variable amplitude loading – Inference and uncertainty estimation. *International Journal of Fatigue*, 135, 105515. https://doi.org/10.1016/j.ijfatigue.2020.105515

Lieurade, H.P., Huther, I. and Lefebvre, F. (2008). Effect of weld quality and post weld improvement techniques on the fatigue resistance of extra high strength steels. *Welding in the World*, 52, 106-115. https://doi.org/10.1007/BF03266658

Liu, Y.C., Leifsson, L., Pietrenko-Dabrowska, A. and Koziel, S. (2022). Analysis of agricultural and engineering systems using simulation decomposition. *International Conference on Computational Science*, pp 435-444. https://doi.org/10.1007/978-3-031-08757-8_36

Mahadevan, S. and Ni, K. (2003). Damage tolerance reliability analysis of automotive spot-welded joints. *Reliability Engineering & System Safety*, 81(1), 9-21. https://doi.org/10.1016/S0951-8320(03)00057-7

Mara, T.A., Tarantola, S. and Annoni, P. (2015). Non-parametric methods for global sensitivity analysis of model output with dependent inputs. *Environmental Modelling & Software*, 72, 173-183. https://doi.org/10.1016/j.envsoft.2015.07.010

Marzban, S. and Lahmer, T. (2016). Conceptual implementation of the variance-based sensitivity analysis for the calculation of the first-order effects. *Journal of Statistical Theory and Practice*, 10(4), 589-611. https://doi.org/10.1080/15598608.2016.1207578

MathWorks. Generating Quasi-Random Numbers. https://se.mathwor

ks.com/help/stats/generating-quasi-random-numbers.html (accessed October 1, 2013).

Menz, M., Dubreuil, S., Morio, J., Gogu, C., Bartoli, N. and Chiron, M. (2021). Variance based sensitivity analysis for Monte Carlo and importance sampling reliability assessment with Gaussian processes. *Structural Safety*, 93, 102116. https://doi.org/10.1016/j.strusafe.2021.102116

Myers, R.H., Montgomery, D.C. and Anderson-Cook, C.M. (2016). *Response Surface Methodology: Process and Product Optimization using Designed Experiments*, John Wiley & Sons. pp 1-859. ISBN: 978-1-118-91601-8

Myers, A., Kozlova, M. and Yeomans, J.S. (2024). Where should we go? Deep tech market entry decisions through the lens of uncertainty. *Sensitivity Analysis for Business, Technology, and Policymaking Made Easy with Simulation Decomposition*, Routledge. pp 142-161. https://doi.org/10.4324/9781003453789-9

Olken, F. and Rotem, D. (1986). Simple random sampling from relational databases. *Proceedings of the 12th International Conference on Very Large Data Bases*, San Francisco, United States.

Owen, A.B. (2020). On dropping the first sobol' point. *International Conference on Monte Carlo and Quasi-Monte Carlo Methods in Scientific Computing*, pp 71-86. https://doi.org/10.1007/978-3-030-98319-2_4

Owen, A.B. (2023). Practical Quasi-Monte Carlo. https://artowen.su.domains/mc/practicalqmc.pdf

Owen, M.P., Panken, A., Moss, R., Alvarez, L. and Leeper, C. (2019). ACAS Xu: Integrated collision avoidance and detect and avoid capability for UAS. *2019 IEEE/AIAA 38th Digital Avionics Systems Conference (DASC)*, San Diego, USA. https://doi.org/10.1109/DASC43569.2019.9081758

Pellegrino, R., Kozlova, M., Brandao, L. and Yeomans, J.S. (2024). Unpacking the role of contextual factors in public support for mitigating revenue risk in public-private partnership projects. *Sensitivity Analysis for Business, Technology, and Policymaking Made Easy with Simulation Decomposition*. Routledge. pp 93-115. https://doi.org/10.4324/ 9781003453789-7

Pérez, M.G., Kozlova, M., Bermúdez, S.I., Pérez, J.C. and Yeomans, J.S. (2024). Sensitivity analysis of a superconducting magnet design model. *Sensitivity Analysis for Business, Technology, and Policymaking Made Easy with Simulation Decomposition*. Routledge. pp 283-327. https://doi.org/10.4324/9781003453789-16

Pleil, J.D., Stiegel, M.A., Madden, M. C. and Sobus, J.R. (2011). Heat map visualization of complex environmental and biomarker measurements. *Chemosphere*, 84(5), 716-723. https://doi.org/10.1016/j.chemosphere.2011.03.017

Plischke, E. (2012). How to compute variance-based sensitivity indicators with your spreadsheet software. *Environmental Modelling & Software*, 35, 188-191. https://doi.org/10.1016/j.envsoft.2012.03.004

prEN 1993-1-14. (2023). *Eurocode 3–Design Of Steel Structures–Part -1-14: Design Assisted by Finite Element Analysis*. European Committee for Standardization. pp 4-48. https://www.phd.eng.br/wp-content/uploads/2015/12/en.1993.1.6.2007.pdf

Puy, A., Beneventano, P., Levin, S. A., Lo Piano, S., Portaluri, T. and Saltelli, A. (2022). Models with higher effective dimensions tend to produce more uncertain estimates. *Science Advances*, 8(42), eabn9450. https://doi.org/10.1126/sciadv.abn9450

Puy, A., Roy, P. and Saltelli, A. (2024). Discrepancy measures for sensitivity analysis in mathematical modeling. *Technometrics*, 66(3), 347-357. https://doi.org/10.1080/00401706.2024.2304341

Razavi, S. and Gupta, H.V. (2016). A new framework for comprehensive, robust, and efficient global sensitivity analysis: 1. Theory. *Water Resources Research*, 52(1), 423-439. https://doi.org/10.1002/2015WR017558

Robbe, P. The QMC module for Julia. https://github.com/PieterjanRobbe/QMC.jl (accessed October 1, 2018).

Ruiz Muñoz, S. and Sorensen, J. (2020). Probabilistic inspection planning of offshore welds subject to the transition from protected to corrosive environment. *Reliability Engineering & System Safety*, 202, 107009. https://doi.org/10.1016/j.ress.2020.107009

Roy, P. and Kozlova, M. (2024). Simulation decomposition in python. *Journal of Open Source Software*. 9(98), 6713. https://doi.org/10.21105/joss.06713

Saltelli, A. (2002). Making best use of model evaluations to compute sensitivity indices. *Computer Physics Communications*, 145(2), 280-297. https://doi.org/10.1016/S0010-4655(02)00280-1

Saltelli, A., Tarantola, S., Campolongo, F. and Ratto, M.. (2004). *Sensitivity Analysis in Practice: A Guide to Assessing Scientific Models*. Chichester, England. pp 1-232.

Saltelli, A., Ratto, M., Andres, T., Campolongo, F., Cariboni, J., Gatelli, D. and Tarantola, S. (2008). *Global Sensitivity Analysis: The Primer*. John Wiley & Sons, pp 1-292. https://doi.org/10.1002/9780470725184

Saltelli, A., Annoni, P., Azzini, I., Campolongo, F., Ratto, M. and Tarantola, S. (2010). Variance based sensitivity analysis of model output, design and estimator for the total sensitivity index. *Computer Physics Communications*, 181(2), 259-270. https://doi.org/10.1016/j.cpc.2009.09.018

Saltelli, A., Aleksankina, K., Becker, W., Fennell, P., Ferretti, F., Holst, N., Li, S. and Wu, Q. (2019). Why so many published sensitivity analyses are false: A systematic review of sensitivity analysis practices. *Environmental Modelling & Software*, 114, 29-39. https://doi.org/10.1016/j.envsoft.2019.01.012

Saltelli, A., Jakeman, A., Razavi, S. and Wu, Q. (2021). Sensitivity analysis: a discipline coming of age. *Environmental Modelling & Software*, 146, 105226. https://doi.org/10.1016/j.envsoft.2021.105226

Saltelli, A. (2023). Sensitivity Analysis Made Easy. *Presentation at Workshop on Modelling*. (accessed on Feb 24 2025)

SciPy. Quasi-Monte Carlo Submodule (scipy.stats.qmc). https://docs.scipy.org/doc/scipy/reference/stats.qmc.html (accessed October 1, 2023).

Shang, X., Su, L., Fang, H., Zeng, B. and Zhang, Z. (2023). An efficient multi-fidelity Kriging surrogate model-based method for global sensitivity analysis. *Reliability Engineering & System Safety*, 229, 108858. https://doi.org/10.1016/j.ress.2022.108858

Shapley, L.S. (1953). A value for n-person games. *Contributions to the Theory of Games II*. Princeton University Press, pp 307-317. https://doi.org/10.1515/9781400881970-018

Shen, X., Feng, K., Xu, H., Wang, G., Zhang, Y., Dai, Y. and Yun, W. (2023). Reliability analysis of bending fatigue life of hydraulic pipeline. *Reliability Engineering & System Safety*, 231, 109019. https://doi.org/10.1016/j.ress.2022.109019

Shi, W., Zhou, Q. and Zhou, Y. (2023). An efficient elementary effect-based method for sensitivity analysis in identifying main and two-factor interaction effects. *Reliability Engineering & System Safety*, 237, 109365. https://doi.org/10.1016/j.ress.2023.109365

Shittu, A.A., Mehmanparast, A. and Hart, P. (2021). Comparative study between S-N and fracture mechanics approach on reliability assessment of offshore wind turbine jacket foundations. *Reliability Engineering & System Safety*, 215, 107838. https://doi.org/10.1016/j.ress.2021.107838

Singh, S. (2003). Simple Random Sampling. *Advanced Sampling Theory with Applications: How Michael 'Selected' Amy Volume I*, Springer Dordrecht, pp 71-136. https://doi.org/10.1007/978-94-007-0789-4_2

Smith, K.N., Watson, P. and Topper, T.H. (1970). A stress-strain function for the fatigue of metals. *Journal of Materials*, 5, 767-778.

Sobol', I.M. (1967). On the distribution of points in a cube and the approximate evaluation of integrals. *Zhurnal Vychislitel'noi Matematiki i Matematicheskoi Fiziki*, 7(4), 784-802. https://doi.org/10.1016/0041-5553(67)90144-9

Sobol', I. M. (1993). Sensitivity analysis for non-linear mathematical models. *Mathematical Modelling and Computational Experiments*,

1, 407-414

Sobol', I.M. (2001). Global sensitivity indices for nonlinear mathematical models and their Monte Carlo estimates. *Mathematics and Computers in Simulation*, 55(1-3), 271-280. https://doi.org/10.1016/S0378-4754(00)00270-6

Sobol', I. and Kucherenko, S. (2010). Derivative based global sensitivity measures. *Procedia-Social and Behavioral Sciences*, 2(6), 7745-7746. https://doi.org/10.1016/j.sbspro.2010.05.208

Sonsino, C.M., Fricke, W., de Bruyne, F., Hoppe, A., Ahmadi, A. and Zhang, G. (2012). Notch stress concepts for the fatigue assessment of welded joints–background and applications. *International Journal of Fatigue*, 34, 2-16. https://doi.org/10.1016/j.ijfatigue.2010.04.011

Suard, S., Hostikka, S. and Baccou, J. (2013). Sensitivity analysis of fire models using a fractional design. *Fire Safety Journal*, 62, 115-124. https://doi.org/10.1016/j.firesaf.2013.01.031

Sudret, B. (2008). Global sensitivity analysis using polynomial chaos expansions. *Reliability Engineering & System Safety*, 93(7), 964-979. https://doi.org/10.1016/j.ress.2007.04.002

Tong, C. (2006). Refinement strategies for stratified sampling methods. *Reliability Engineering & System Safety*, 91(10-11), 1257-1265. https://doi.org/10.1016/j.ress.2005.11.027

Vinitskaia, N., Zaikova, A., Kozlova, M. and Yeomans, J.S. (2024). Uncertainty considerations in life cycle assessment of COVID-19 masks: Single-use versus reusable. *Sensitivity Analysis for Business, Technology, and Policymaking Made Easy with Simulation Decomposition*. Routledge, pp 165-188. https://doi.org/10.4324/9781003453789-11

Vuillod, B., Montemurro, M., Panettieri, E. and Hallo, L. (2023). A comparison between Sobol's indices and Shapley's effect for global sensitivity analysis of systems with independent input variables. *Reliability Engineering & System Safety*, 234, 109177. https://doi.org/10.1016/j.ress.2023.109177

Wang, Z. and Jia, G. (2023). Extended sample-based approach for efficient sensitivity analysis of group of random variables. *Reliability Engineering & System Safety*, 231, 108991. https://doi.org/10.1016/j.ress.2022.108991

Ye, Y., Yang, Q., Zhang, J., Meng, S. and Wang, J. (2023). A dynamic data driven reliability Prognosis method for structural digital twin and experimental validation. *Reliability Engineering & System Safety*, 240, 109543. https://doi.org/10.1016/j.ress.2023.109543

Yeomans, J.S. (2020). Computational analytics for supporting environmental decision-making and analysis: An introduction. *Journal of Environmental Informatics Letters*, 4(2), 48-49. https://doi.org/10.3808/jeil.202000040

Ziehn, T. and Tomlin, A.S. (2009). GUI–HDMR–A software tool for global sensitivity analysis of complex models. *Environmental Modelling & Software*, 24(7), 775-785. https://doi.org/10.1016/j.envsoft.2008.12.002